JOURNAL OF VIROLOGY, Jan. 1990, p. 339–346
0022-538X/90/010339-08$02.00/0

Vol. 64, No. 1

Intracellular Transport of Recombinant Coronavirus Spike Proteins: Implications for Virus Assembly

H. VENNEMA, L. HEIJNEN, A. ZIJDERVELD, M. C. HORZINEK, AND W. J. M. SPAAN*

Institute of Virology, Department of Infectious Diseases and Immunology, Veterinary Faculty, State University, Yalelaan 1, P. O. Box 80.165, 3508 TD Utrecht, The Netherlands

Received 14 July 1989/Accepted 25 September 1989

Coronavirus spike protein genes were expressed in vitro by using the recombinant vaccinia virus expression system. Recombinant spike proteins were expressed at the cell surface and induced cell fusion in a host-cell-dependent fashion. The intracellular transport of recombinant spike proteins was studied. The half time of acquisition of resistance to endo-β-*N*-acetylglucosaminidase H was approximately 3 h for the recombinant feline infectious peritonitis virus S protein. The S protein in feline infectious peritonitis virus-infected cells was found to have a half time of acquisition of resistance to endo-β-*N*-acetylglucosaminidase H of approximately 1 h. This difference can be explained by the fact that coronavirus budding takes place at intracellular membranes and that the oligosaccharides of the spike protein are modified after budding. Apparently, spike protein incorporated into budded virions is transported faster through the Golgi apparatus than is spike protein alone. These findings provide new insights into the mechanism of coronavirus budding and are discussed in relation to current models of intracellular transport and sorting of proteins.

Coronaviruses are enveloped positive-stranded RNA viruses. Virions of most coronaviruses contain three proteins: the phosphorylated nucleocapsid protein N; a small glycoprotein, M, which is largely embedded in the membrane; and a large glycoprotein, S, which forms petal-shaped peplomers (26). Both glycoproteins are synthesized on ribosomes bound to the rough endoplasmic reticulum (RER) (18).

An interesting aspect of coronavirus replication is the intracellular budding of virions, which takes place in transitional elements between the endoplasmic reticulum and pre-Golgi (31). The M protein accumulates in the Golgi apparatus and is believed to determine the site of budding (28). Intracellular accumulation is an intrinsic property of the M protein and does not require the presence of other viral components (13, 24).

The S protein mediates binding of virions to the host cell receptor, causes cell fusion, and is the major target for virus-neutralizing antibodies. Analysis of the primary nucleotide sequence and the predicted amino acid sequence of S proteins of several coronaviruses revealed features typical of type I membrane proteins (26). The biosynthesis of S has only been studied in coronavirus-infected cells. The S protein is cotranslationally glycosylated (26, 28). During virus maturation the N-linked oligosaccharides of S undergo Golgi-specific modifications (18). Mature virions are released from the cell through the constitutive exocytic pathway (30). A proportion of S that is not incorporated into virions is transported to the plasma membrane, where it induces cell-to-cell fusion (28). Hence, two populations of S protein are transported through the exocytic pathway: S protein anchored in cellular and S protein anchored in viral membranes. Neither the ratio nor the kinetics of intracellular transport of these two populations of S protein are known.

In the present study we have used vaccinia virus recombinants expressing S genes of three different coronaviruses to study the biosynthesis of S protein in the absence of virus budding. We found that it reached the plasma membrane and that it induced cell fusion but that transport through the Golgi apparatus occurred with extremely slow kinetics. Comparison with results from coronavirus-infected cells showed that S protein was transported much faster once it had been incorporated into virions. The implications of these findings are discussed in relation to models of coronavirus budding and protein targeting.

MATERIALS AND METHODS

Cells and viruses. Coronavirus strains used were feline infectious peritonitis virus (FIPV) strain 79-1146 (16), mouse hepatitis virus (MHV) strain A59, and infectious bronchitis virus (IBV) strain M42.

Cells were maintained as monolayer cultures in Dulbecco modified Eagle medium (GIBCO Laboratories) containing 10% heat-inactivated fetal bovine serum and 100 IU of penicillin and 100 μg of streptomycin per ml. For FIPV infections, *Felis catus* whole fetus (fcwf-D), Norden Laboratories feline kidney (NLFK), and Crandell feline kidney (CrFK) cells were used. For MHV infections Sac^- and L cells were used, and Vero cells were used for IBV. Vaccinia virus (strain WR) infections were performed with the same cell lines and in addition using HeLa, human 143 thymidine kinase-negative (TK^-), and rabbit kidney (RK-13) cells.

Recombinant DNA techniques. Cloning procedures were as described by Maniatis et al. (15). Enzymes were used according to the specifications of the manufacturers (Pharmacia, New England BioLabs, and Boehringer Mannheim Biochemicals).

Cloning of full-length spike protein genes in vaccinia virus insertion vectors. The S genes of FIPV 79-1146, MHV A59, and IBV M41 have been cloned and sequenced in our laboratory (3, 12, 20).

The coding sequence of the FIPV S gene was recloned from cDNA clone B1 as described previously (4). The complete coding sequence was isolated as a 4.5-kilobase (kb) *Bam*HI fragment and ligated to *Bam*HI-cut transfer vector pGS20 (14).

The full-length coding region of the S gene of MHV A59 was reconstructed from two overlapping cDNA clones, B24 and F11 (12). Sequences upstream of the initiation codon

* Corresponding author.

were deleted in a way similar to that described previously for the FIPV S gene (4). A 1.5-kb *Pst*I fragment of clone F11 was recloned in the *Pst*I site of M13 mp8. Single-stranded DNA containing the noncoding strand was annealed to synthetic oligonucleotide 5′ CTAAACATGCTGTTC 3′, which contains the translation initiation codon (underlined). This oligonucleotide was used as a primer to synthesize the complementary strand with Klenow DNA polymerase. A double-stranded fragment of the 5′ end of the coding region was obtained by sequential digestion with S1 nuclease and *Pst*I. The resulting fragment was purified and ligated to *Pst*I- and *Hin*cII-digested Bluescribe plasmid, yielding plasmid BSM1F11. This plasmid contains a unique *Cla*I site in the area that overlaps with the insert of clone B24 and a *Bam*HI site at the 5′ end of the gene. The *Hin*dIII site of the polylinker sequence of cDNA clone B24 was converted to a *Sal*I site by linker addition, yielding plasmid B24S. To reconstruct the complete coding sequence, the 1.1-kb *Bam*HI-*Cla*I fragment from BSM1F11 was ligated together with the 3.5-kb *Cla*I-*Sal*I fragment of B24S in a three-fragment ligation to *Bam*HI- and *Sal*I-digested Bluescribe plasmid, yielding BSE2. Finally, the unique *Sal*I site of BSE2 was converted into a *Bam*HI site by linker addition. The entire S gene coding region of MHV was isolated from the final construct, designated pDGE2, as a 4.6-kb *Bam*HI fragment and ligated to *Bam*HI-digested pGS20.

The coding sequence of the S gene of IBV M41 was isolated from cDNA clone 39 (20). The unique *Tth*111I site, located 42 base pairs upstream of the initiating AUG codon and the unique *Xba*I site, located 163 base pairs downstream of the termination codon, were converted to *Xho*I sites by linker addition. The resulting fragment was digested with *Xho*I, filled with the Klenow fragment, and ligated to *Sma*I-digested transfer vector pSC11 (1).

The vesicular stomatitis virus (VSV) G coding region was isolated from plasmid pSVGL11, a derivative of pSVGL (22), as a 1.7-kb *Xho*I fragment. This fragment was filled with the Klenow fragment and ligated to *Sma*I-digested pSC11.

Isolation of vaccinia virus recombinants. Recombinant vaccinia viruses were constructed by established procedures (1, 14). Briefly, HeLa cells were infected at low multiplicity of infection with wild-type vaccinia virus strain WR and transfected with the different recombinant transfer plasmids described above. Progeny virus was plaqued on human 143 TK^- cells in the presence of 5-bromodeoxyuridine (25 μg/ml). Recombinant vaccinia viruses were identified by DNA hybridization using specific probes, by dot-blot enzyme-linked immunosorbent assay with specific antisera, or, in the case of pSC11-derived plasmids, by direct visual screening with 5-bromo-4-chloro-3-indolyl-β-D-galactopyranoside. Plaque purification and screening were repeated once or twice before stocks of recombinant viruses were made in HeLa or RK-13 cells.

Infections and metabolic labeling. FIPV infection was carried out in NLFK cells at a multiplicity of infection of 10 50% tissue culture infective doses. Subconfluent monolayers of NLFK or HeLa cells were infected with different vaccinia virus recombinants at a multiplicity of infection of 10 PFU. Protein labeling was carried out at the times indicated below or in the legends in methionine-free medium supplemented with L-[^{35}S]methionine (>1,000 Ci/mmol; Amersham Corp.) at a concentration of 0.1 mCi/ml. Before pulse-labeling, cultures were incubated in methionine-free medium. In some cases a pulse-labeling period was followed by a chase with medium containing 4 mM methionine and 10% fetal calf serum. Cells were lysed in 20 mM Tris hydrochloride (pH 7.5)–1 mM EDTA–100 mM NaCl (TESV) containing 1% Triton X-100 and 2 mM phenylmethylsulfonyl fluoride (0.3 ml/10^6 cells). Released virions in the medium of FIPV-infected NLFK cells were solubilized by adding TESV, Triton X-100, and phenylmethylsulfonyl fluoride from concentrated stock solutions to the same final concentrations as in the cell lysates.

RIP and endo H analysis. Radio immunoprecipitation (RIP) with ascitic fluid (A36) of an FIPV-infected cat were carried out overnight at 4°C in TESV containing 0.4% Triton X-100 at a 600-fold dilution for lysates of recombinant vaccinia virus-infected cells and at a 100-fold dilution for lysates of FIPV- and mock-infected cells. For immunoprecipitation of the MHV S, IBV S, and VSV G proteins, sera of rabbits hyperimmunized with the respective viruses were used. After the addition of KCl (0.5 M), the immune complexes were bound to Pansorbin (Calbiochem) for 2.5 h at 4°C and subsequently pelleted by centrifugation. Pellets were washed three times in TESV containing 0.1% Triton X-100 and finally suspended in 50 mM Tris hydrochloride (pH 6.8) containing 0.25% sodium dodecyl sulfate and boiled for 2 min to dissolve immune complexes. Immunoprecipitated proteins were digested with endo-β-*N*-acetylglucosaminidase H (endo H; Boehringer Mannheim Biochemicals) as follows: to 10 μl of dissolved immunoprecipitate 15 μl of 150 mM sodium citrate buffer (pH 5.3) was added, and the mixture was incubated overnight at 37°C in the absence or presence of 1 mU of endo H. Laemmli sample buffer was then added, and the samples were analyzed in sodium dodecyl sulfate–10% polyacrylamide gels (10).

Indirect immunofluorescence test. For surface immunofluorescence, RK-13 cells seeded on glass cover slips were infected at a multiplicity of infection of 1 PFU. At 16 h postinfection (p.i.), cells were washed with phosphate-buffered saline (PBS) and incubated with antiserum at 4°C for 1.5 h. For MHV and IBV S proteins and VSV G protein, the same antisera were used as in the RIPs. The ascitic fluid used for the FIPV S protein RIP was poorly reactive in an indirect immunofluorescence assay; therefore, serum of a kitten after experimental infection with the homologous FIPV strain was used in this assay. All antisera were used at a 100-fold dilution. After incubation with the first antiserum, cells were washed extensively with PBS. Fluorescein isothiocyanate-conjugated goat anti-rabbit or rabbit anti-cat immunoglobulin G (Fc and Fab, respectively; Nordic Immunology) were used at a 100-fold dilution with similar incubation as for the primary antisera. After extensive washing with PBS, the cells were fixed with 4% formaldehyde in PBS for 30 min at room temperature and washed again with PBS. Cover slips were mounted with 90% glycerol solution in PBS containing 25 mg of 1,4-diazabicyclo-(2,2,2)-octane (Sigma Chemical Co.) per ml prepared as described previously (8).

RESULTS

Expression of recombinant FIPV S protein. Recombinant vaccinia virus encoding the FIPV S protein under control of the vaccinia virus 7.5-kilodalton promoter was constructed and designated vFS. To examine the S protein encoded by vFS, NLFK cells were infected with the recombinant vaccinia virus, wild-type vaccinia virus (vWR), or FIPV or mock infected. Infected cells were labeled with L-[^{35}S] methionine for 30 min at 8 h p.i. (FIPV- and mock-infected cells) or at 16 h p.i. (vWR- and vFS-infected cells). Radioactively labeled proteins were incubated with polyclonal anti-FIPV ascitic fluid and analyzed by sodium dodecyl

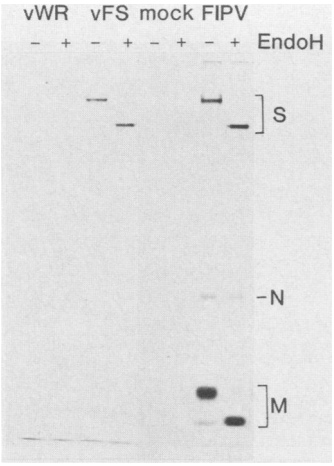

FIG. 1. RIP and sodium dodecyl sulfate-polyacrylamide gel electrophoretic analysis of recombinant FIPV S protein. Recombinant (vFS) and wild-type (vWR) vaccinia virus-infected cells were labeled for 30 min at 16 h p.i. with [^{35}S]methionine; FIPV- and mock-infected cells were labeled in the same way at 8 h p.i. RIP was carried out with ascitic fluid containing polyclonal anti-FIPV antibodies. FIPV structural proteins (S, N, and M) are indicated. Immunoprecipitates were split in two samples; one half was mock treated, and the other was treated with endo H (− and +, respectively). Treatment with endo H resulted in a shift to a higher electrophoretic mobility of the recombinant and the FIPV S and M proteins.

sulfate-polyacrylamide gel electrophoresis (Fig. 1). From the lysate of FIPV-infected cells, the S protein, the N protein, and two forms of the M protein were precipitated. In cells infected with vFS a protein was detected which comigrated with the FIPV S protein and which was absent from vWR- or mock-infected cells. Endo H treatment of the immunoprecipitates resulted in an equal reduction in apparent molecular weight of the S protein derived from FIPV- and vFS-infected cells. In protein labeled for 30 min, no endo H-resistant material was detected, indicating that the acquisition of endo H resistance is rather slow as compared with resistance to the VSV G protein (see below). These experiments show that viral and recombinant FIPV S proteins are indistinguishable with respect to size and glycosylation. Similarly, recombinant vaccinia viruses expressing the S protein of MHV and IBV (designated vMS and vIS, respectively) were constructed and analyzed. Again, no difference in electrophoretic mobility between the recombinant S proteins and the respective viral proteins was observed (data not shown).

Cell surface expression and biological activity of recombinant S proteins. To assay the cell surface expression in recombinant vaccinia virus-infected cells the S proteins to FIPV, MHV, and IBV were visualized by indirect immunofluorescence. Surface immunofluorescence was detected with all three recombinant S proteins (Fig. 2a, c, and e). For comparison, cells infected with a recombinant vaccinia virus expressing the VSV G protein (vVG) were processed in the same way and showed similar surface staining (Fig. 2g). With each antiserum wild-type vaccinia virus (vWR)-infected cells showed only background staining (Fig. 2b, d, f, and h). Similar results have been shown previously for the S protein of IBV strain M42 (29).

In coronavirus-infected cells, S protein expressed on the cell surface is believed to induce cell-cell fusion (28). This is indeed the case, as became evident from the appearance of large syncytia in vFS-infected NLFK cells and vMS-infected Sac$^-$ cells (Fig. 3a and c). No syncytium formation was observed in NLFK or Sac$^-$ cells infected with wild-type vaccinia virus (Fig. 3b and d) or with vIS (data not shown). Induction of cell fusion by recombinant vFS was restricted to cells of feline origin, and that by vMS was restricted to murine cells.

These data show that the recombinant S protein is expressed on the cell surface and that it retains biological activity.

Intracellular transport of recombinant S proteins. During the transport from the RER to the *trans*-Golgi cisterna the oligosaccharide side chains of N-glycosylated glycoproteins are processed and modified. As a result of these modifications, the cotranslationally added high-mannose side chains, which are endo H sensitive, become endo H resistant in the medial Golgi cisterna (6). Therefore, the rate of acquisition of endo H resistance can be used to study the kinetics of intracellular transport from the endoplasmic reticulum to the medial Golgi. No endo H-resistant material was produced during a 30-min pulse (Fig. 1), indicating a slow transport. To determine the rate of acquisition of endo H resistance, NLFK cells were infected with vFS and pulse-labeled for 30 min at 16 h p.i. After chases for different times, cell lysates were prepared, and labeled S protein was immunoprecipitated and digested with endo H (Fig. 4). In the pulse-labeled sample and during the first chase period of 1 h, no endo H-resistant material was detected. As a result of longer chase periods, the intensity of the gp200 band gradually decreased, whereas a protein with a slightly higher molecular weight appeared (gp220). This shift in apparent molecular weight probably reflects Golgi modifications, particularly sialylation. The higher-molecular-weight form is resistant to digestion by endo H, albeit not completely. Apparently the mature S protein contains both endo H-resistant and endo H-sensitive oligosaccharides, as has been observed previously for the S protein of MHV A59 (18). In accordance with current terminology (5), we call this incomplete resistance maximal endo H resistance.

After a 3-h chase period about half of the recombinant S protein of FIPV was still sensitive to digestion by endo H. The other half was partly converted to the mature (sialylated) form and to an intermediate endo H-resistant form that migrated as a discrete band of intermediate mobility. Sometimes, *cis* and medial Golgi processing intermediates, which are digested less efficiently than RER forms, were detected as a smear. As expected, only the mature, maximally endo H-resistant form was detected after surface immunoprecipitation of metabolically labeled intact vFS-infected cells (data not shown).

To assay whether the S proteins of the other coronaviruses were transported with similar kinetics, vMS and vIS were analyzed in infected NLFK cells. In addition, vVG was included in this study. Figure 5 shows the results of an experiment with a 30-min pulse-labeling at 12 h p.i., followed by a 60-min chase period. None of the three coronavirus S proteins showed detectable acquisition of resistance to endo H within the 60-min chase period. The VSV G protein was processed much faster: already at the end of the 30-min pulse it was partially resistant to endo H. The pulse-labeled untreated G protein was separated into two bands, of which the upper band represents the terminally sialylated form (9). After the 60-min chase period, all of the VSV G protein was converted to this form and was resistant to endo H.

In the lanes containing the proteins of the vMS lysates, in addition to the S protein, two background bands could be seen which were also precipitated from lysates of wild-type

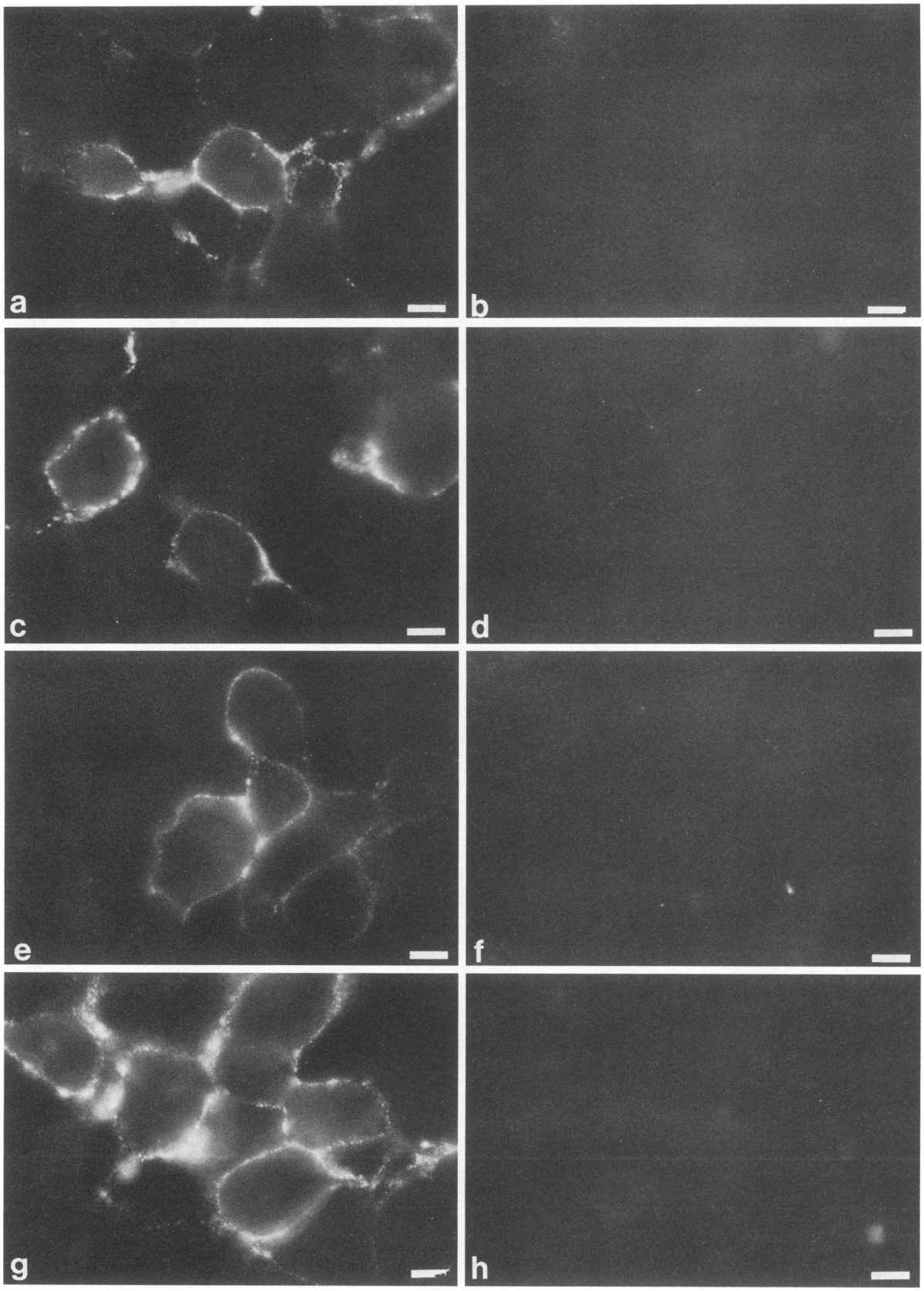
a
b
c
d
e
f
g
h

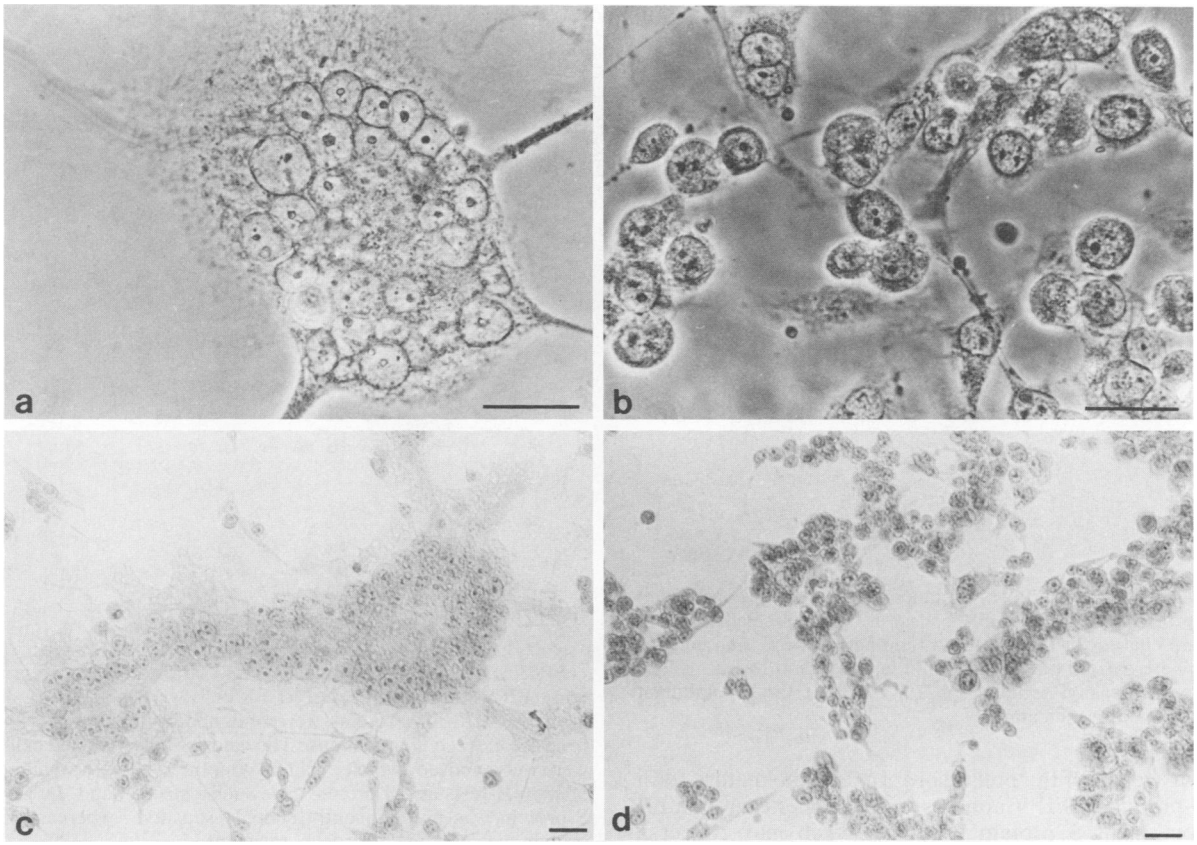

FIG. 3. Biological activity of recombinant S proteins. NLFK cells, used for propagation of FIPV, were infected with recombinant vaccinia virus vFS (a) and with wild-type vaccinia virus strain WR (b). Infected NLFK cells were photographed by using dark-field microscopy (magnification, ×400). Sac$^-$ cells, employed for growing MHV, were infected with recombinant vaccinia virus vMS (c) and with wild-type vaccinia virus strain WR (d). Infected Sac$^-$ cells were stained for nuclei by using hematoxylin and photographed under light microscopy (magnification, ×100). Bars, 5 μm. Recombinant vaccinia viruses induced the formation of large multinucleated syncytia, whereas rounding of cells was seen in wild-type vaccinia virus cells.

vaccinia virus-infected cells (data not shown). At the end of the pulse-labeling, the protein of the upper background band was almost completely sensitive to endo H, and after the 60-min chase it was endo H resistant, similar to the VSV G protein.

Since the VSV G protein was expressed in the same way as the coronavirus S proteins, the observed phenomenon of slow intracellular transport is indeed coronavirus specific and not the result of the expression system used. Although an accurate estimate cannot be made due to the relatively long pulse labeling, the intracellular transport rate of VSV G protein in our system appears to be comparable to the rate observed in VSV-infected cells (9) and in cells expressing the protein from cloned cDNA (23).

The data show that in the absence of other viral components coronavirus S proteins are slowly transported from the RER to the medial Golgi compartment, as measured by the rate of acquisition of resistance to digestion by endo H.

Biosynthesis of the S protein in FIPV-infected cells. To study the biosynthesis of S in FIPV-infected cells, we analyzed the structural proteins in cell lysates and of virions released into the extracellular medium. FIPV-infected NLFK cells were labeled with [^{35}S]methionine for 20 min at 5 h p.i. Cell lysates were prepared immediately or after chase periods of 1 and 3 h. The medium of infected cells was harvested after a 3-h chase period. The oligosaccharides of the S protein from cell lysates were predominantly endo H sensitive at all times (Fig. 6). At later chase times a smear of partially resistant forms was detected. The M protein was present as the glycosylated endo H-sensitive form, with relatively small amounts of both endo H-resistant and unglycosylated forms. The amount of intracellular protein gradually decreased during the chase as a result of virus release. The virion S protein had a slightly higher apparent molecular weight than the intracellular protein and was maximally endo H resistant. The difference in apparent

FIG. 2. Cell surface expression of recombinant S proteins. RK-13 cells seeded on glass cover slips were infected with recombinant vaccinia virus vFS (a), vMS (c), vIS (e), and vVG (g) or with wild-type vaccinia virus strain WR (b, d, f, and h) and processed for indirect immunofluorescence at 16 h p.i. Cells infected with recombinant vaccinia viruses were incubated with the homologous antiserum. Samples of wild-type vaccinia virus-infected cells were incubated with each antiserum as negative controls. Pairs of samples incubated with the same antiserum are shown next to each other. Bars, 2 μm. Recombinant vaccinia virus-infected cells showed distinct surface staining, whereas only background staining was seen in wild-type vaccinia virus-infected cells.

FIG. 4. Kinetics of endo H resistance acquisition of recombinant FIPV S protein. Infected NLFK cells were pulse-labeled 16 h p.i. for 1 h and chased for the indicated time periods. RIP and endo H analyses were carried out as described in the legend to Fig. 1. The precursor (gp200) and product (gp220) forms of the recombinant FIPV S protein are indicated.

molecular weight of the precursor form and the mature form of the S protein of FIPV appears to be smaller than that for the recombinant S protein (Fig. 4), which may reflect a difference in the extent of sialylation. Because of the qualitative differences in endo H sensitivity, in particular of the S protein, between cell lysates and released virions, we concluded that additional purification of virions was not necessary.

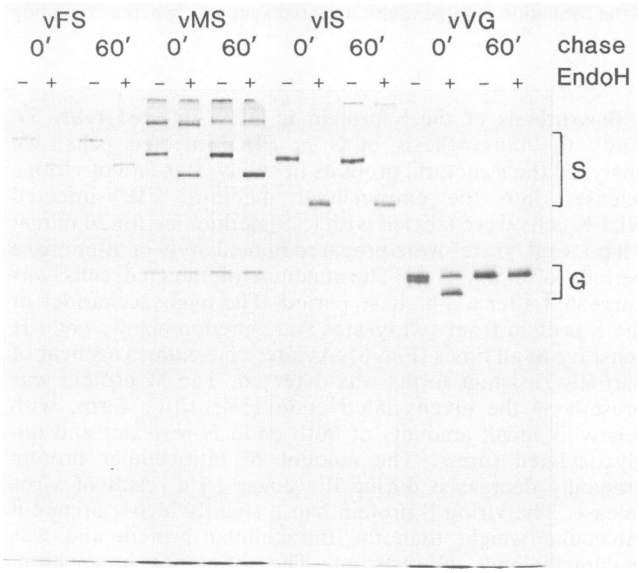

FIG. 5. Endo H analysis of three different recombinant coronavirus S proteins and of recombinant VSV G protein. Infected NLFK cells were pulse-labeled at 12 h p.i. for 30 min and lysed immediately or after a chase of 1 h. Recombinant vaccinia viruses are indicated above each panel of four lanes. RIP with specific antisera, followed by endo H digestion, was carried out as described in the legend to Fig. 1. Recombinant S proteins remained endo H sensitive, and the recombinant VSV G protein became completely endo H resistant during the 1-h chase period.

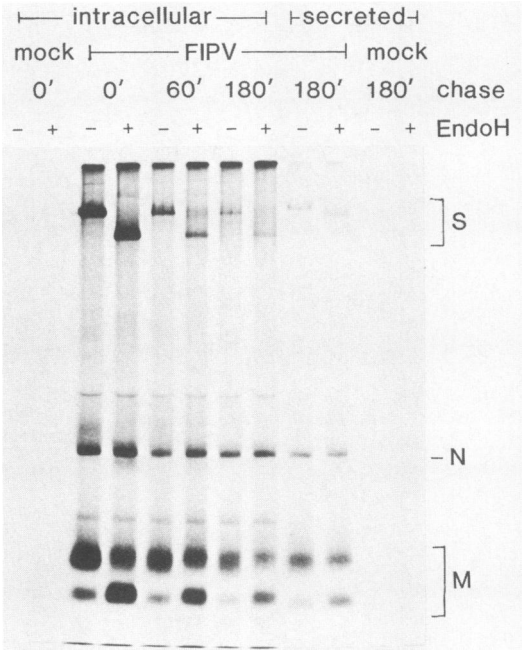

FIG. 6. Analysis of intracellular and virion FIPV structural proteins. FIPV- or mock-infected NLFK cells were labeled as indicated in the text. Virion proteins were obtained by immunoprecipitation from the extracellular medium. The lanes of pulse-labeled cell lysate were overexposed, which explains why the relatively small amount of endo H-resistant M protein gave such a strong band. Intracellular S protein was predominantly endo H sensitive, whereas virion S protein was maximally endo H resistant.

Next, the rate of acquisition of resistance to endo H digestion of the FIPV S protein was determined. As shown above, the S protein of released virus was resistant to endo H. Omission of secreted endo H resistant protein from the assay would lead to serious underestimation of the rate of acquisition of resistance to endo H (34). Therefore, lysates containing both the intracellular and the secreted material were prepared by adding concentrated lysis buffer and protease inhibitor to a culture dish without removing the medium. FIPV-infected NLFK cells were pulse-labeled for 30 min 9 h p.i. and chased for different periods (Fig. 7). More than half of the S protein had become maximally resistant to digestion by endo H after a chase period of 1 h. The amount of endo H-sensitive material gradually decreased. A small amount of endo H-sensitive material remained after a 3-h chase period. The FIPV M protein was not completely glycosylated and did not become totally endo H resistant. The maximum level of endo H resistance was reached during the first 30 min.

The results in the last section indicate that the rate-limiting step in intracellular transport and release of the FIPV S protein is the step prior to the acquisition of endo H resistance, since cell lysates contain only very little partially endo H resistant material.

DISCUSSION

In this report we have shown that S proteins of several coronaviruses were expressed at the cell surface of recom-

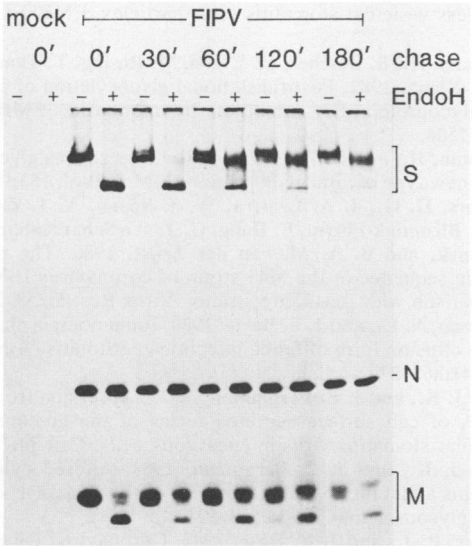

FIG. 7. Kinetics of endo H resistance acquisition of the S protein in FIPV-infected NLFK cells. Metabolic labeling was carried out at 9 h p.i. for 30 min. Lysates were prepared immediately or after the indicated chase times. Intracellular and virion proteins were analyzed together in combined lysates, prepared by adding concentrated lysis buffer to the medium of infected cells. RIP and endo H analyses were carried out as described in the legend to Fig. 1. Structural proteins are indicated. In combined lysates more than half of the labeled S protein was endo H resistant after 1 h.

binant vaccinia virus-infected cells but remained completely endo H sensitive for at least 1 h after synthesis. Also, the recombinant S protein of FIPV became resistant to digestion by endo H with a half time of more than 3 h; similar kinetics were observed for the recombinant S proteins of MHV and IBV (data not shown). In contrast, the S protein in FIPV-infected cells became endo H resistant with a half time of less than 1 h. The same results were obtained when this comparison was made for MHV (unpublished observations).

This retardation between the RER and medial Golgi, in the absence of virus budding, may be interpreted as a transient accumulation at or near the site of budding. This transient accumulation may enable efficient incorporation into virions or determine the site of the budding event. Recently it was shown that budding of MHV takes place in transitional elements between the RER and *cis*-Golgi (31). The morphogenesis of FIPV was typical for a coronavirus (32), and electron microscopy studies have shown that FIPV is assembled at smooth endoplasmic reticulum membranes (21). This intracellular assembly site is thought to be determined by the M protein. However, the MHV M protein accumulates in the Golgi compartment, both in infected cells and in cells expressing recombinant M protein (24). Furthermore, the rate of O glycosylation and terminal sialylation of the M protein, i.e., transport to *trans*-Golgi, is the same in infected and in transfected cells (24), indicating that the MHV M protein is not specifically retarded at the site of budding. The recombinant M protein of IBV, which is N glycosylated, also accumulates in the Golgi apparatus but remains endo H sensitive (13). No data concerning the targeting of the FIPV M protein are available yet. We have observed that S is retarded between the RER and medial Golgi in the absence of virus budding; this suggests that the role of defining the site of budding may also be ascribed to S, particularly in the case of MHV. Further experiments are required to determine the site of retardation more precisely and to explore possible differences between the budding mechanisms of coronaviruses with O- or N-linked glycosylated M proteins.

Treatment of coronavirus-infected cells with the drug tunicamycin results in spikeless virions (7, 19, 25, 27); this observation does not rule out the possibility that the spike protein is involved in the budding mechanism. As was pointed out before (27) and was recently shown for VSV (17), spikeless virions can arise by degradation of the ectodomain of the spike protein after budding. The residual membrane anchor peptides that have been identified for VSV (2, 17) have not yet been found for coronaviruses.

The coronavirus S protein is transported extremely slowly when compared with, e.g., the VSV G protein. Intracellular transport rates can be highly variable, even for closely related membrane glycoproteins (33). In a recent review by Lodish (11), several models were proposed to explain differences in transport rates. They involve putative receptors for either transport or retention or both that interact with signals carried by proteins. Differential transport would be the result of differences in affinity for receptors. We found that S protein in FIPV- and MHV-infected cells is transported faster than the recombinant S protein as measured by oligosaccharide processing. In coronavirus-infected cells, carbohydrate side chains of the S protein can be processed after incorporation into virions. We conclude that incorporated S protein is transported faster than unincorporated S protein and that incorporation is quite efficient.

The recombinant S protein is transported to the plasma membrane as shown by the indirect immunofluorescence test data and the induction of cell fusion. This intrinsic property of the S protein may be responsible also for the transport of virus particles. We propose that the S protein carries putative transport signals located in the ectodomain of the protein and putative retention signals in the cytoplasmic tail. The retardation of S would then be the result of transport and retention. Once the S protein is incorporated into virions, the putative retention signals are no longer recognized and the putative transport signals direct efficient transport along the secretory pathway. Alternatively, virions may be carried with the bulk flow after putative retention signals are shielded, or putative transport signals may be communicated to the ectodomain by binding of other viral components to the S protein. Experiments to identify such signals are in progress.

Our cell fusion data suggest a relationship between cell susceptibility for each coronavirus and the ability of the respective S protein to induce cell-to-cell fusion. Recombinant vaccinia viruses now offer the possibility of testing factors influencing cell fusion, independent of coronavirus replication.

ACKNOWLEDGMENTS

We thank Arnoud van der Spoel and Dirk Geerts for recloning the IBV and MHV S genes, B. Moss for supplying the vectors pGS20 and pSC11, G. Wertz and J. K. Rose for providing wild-type vaccinia virus strain WR and plasmid pSVGL11, respectively, and N Pedersen and R. Sharpie for giving fcwf-D cells and NLFK cells, respectively. We also thank Peter Rottier for helpful discussions and Ewan Chirnside for reviewing the manuscript.

This work was supported by a grant from Duphar BV, Weesp, The Netherlands.

LITERATURE CITED

1. **Chakrabarti, S., K. Brechling, and B. Moss.** 1985. Vaccinia virus expression vector: coexpression of β-galactosidase provides

visual screening of recombinant virus plaques. Mol. Cell. Biol. **5**:3403–3409.

2. **Chen, S. S.-L., N. Ariel, and A. S. Huang.** 1988. Membrane anchors of vesicular stomatitis virus: characterization and incorporation into virions. J. Virol. **62**:2552–2556.
3. **De Groot, R. J., J. Maduro, J. A. Lenstra, M. C. Horzinek, B. A. M. van der Zeijst, and W. J. Spaan.** 1987. cDNA cloning and sequence analysis of the gene encoding the peplomer protein of feline infectious peritonitis virus. J. Gen. Virol. **68**:2639–2646.
4. **De Groot, R. J., R. W. Van Leen, M. J. M. Dalderup, H. Vennema, M. C. Horzinek, and W. J. M. Spaan.** 1989. Stably expressed FIPV peplomer protein induces cell fusion and elicits neutralizing antibodies in mice. Virology **171**:493–502.
5. **Doyle, C., J. Sambrook, and M.-J. Gething.** 1986. Analysis of progressive deletions of the transmembrane and cytoplasmic domains of influenza hemagglutinin. J. Cell Biol. **103**:1193–1204.
6. **Dunphy, W. G., and J. E. Rothman.** 1985. Compartmental organization of the Golgi stack. Cell **42**:13–21.
7. **Holmes, K. V., E. W. Doller, and L. S. Sturman.** 1981. Tunicamycin resistant glycosylation of a coronavirus glycoprotein: demonstration of a novel type of viral glycoprotein. Virology **115**:334–344.
8. **Johnson, G. D., R. S. Davidson, K. C. McNamee, G. Russell, D. Goodwin, and E. J. Holborow.** 1982. Fading of immunofluorescence during microscopy: a study of the phenomenon and its remedy. J. Immunol. Methods **55**:231–242.
9. **Knipe, D. M., H. F. Lodish, and D. Baltimore.** 1977. Localization of two cellular forms of the vesicular stomatitis viral glycoprotein. J. Virol. **21**:1121–1127.
10. **Laemmli, U. K.** 1970. Cleavage of structural proteins during assembly of the head of bacteriophage T4. Nature (London) **227**:680–685.
11. **Lodish, H. F.** 1988. Transport of secretory and membrane glycoproteins from the rough endoplasmic reticulum to the Golgi. J. Biol. Chem. **263**:2107–2110.
12. **Luytjes, W., L. S. Sturman, P. J. Bredenbeek, J. Charité, B. A. M. van der Zeijst, M. C. Horzinek, and W. J. Spaan.** 1987. Primary structure of the glycoprotein E2 of coronavirus MHV-A59 and identification of the trypsin cleavage site. Virology **161**:479–487.
13. **Machamer, C. E., and J. K. Rose.** 1987. A specific transmembrane domain of a coronavirus E1 glycoprotein is required for its retention in the Golgi reaction. J. Cell Biol. **105**:1205–1214.
14. **Mackett, M., G. L. Smith, and B. Moss.** 1984. General method for production and selection of infectious vaccinia virus recombinants expressing foreign genes. J. Virol. **49**:857–864.
15. **Maniatis, T., E. F. Fritsch, and J. Sambrook.** 1982. Molecular cloning: a laboratory manual. Cold Spring Harbor Laboratory, Cold Spring Harbor, N.Y.
16. **McKeirnan, A. J., J. F. Evermann, A. Hargis, and R. L. Ott.** 1981. Isolation of feline coronaviruses from two cats with diverse disease manifestations. Feline Prac. **11**:17–20.
17. **Metsikkö, K., and K. Simons.** 1986. The budding mechanism of spikeless vesicular stomatitis virus particles. EMBO J. **5**:1913–1920.
18. **Niemann, H., B. Boschek, D. Evans, M. Rosing, T. Tamura, and H. D. Klenk.** 1982. Posttranslational glycosylation of coronavirus glycoprotein E1: inhibition by monensin. EMBO J. **1**: 1499–1504.
19. **Niemann, H., and H.-D. Klenk.** 1981. Coronavirus glycoprotein E1, a new type of viral glycoprotein. J. Mol. Biol. **153**:993–1010.
20. **Niesters, H. G., J. A. Lenstra, W. J. Spaan, A. J. Zijderveld, N. M. Bleumink-Pluym, F. Hong, G. J. van Scharrenburg, M. C. Horzinek, and B. A. M. van der Zeijst.** 1986. The peplomer protein sequence of the M41 strain of coronavirus IBV and its comparison with Beaudette strains. Virus Res. **5**:253–263.
21. **Pedersen, N. C., and J. F. Boyle.** 1980. Immunologic phenomena in the effusion form of feline infectious peritonitis. Am. J. Vet. Res. **41**:868–876.
22. **Rose, J. K., and J. E. Bergmann.** 1982. Expression from cloned cDNA of cell surface secreted forms of the glycoprotein of vesicular stomatitis virus in eucaryotic cells. Cell **30**:753–762.
23. **Rose, J. K., and J. E. Bergmann.** 1983. Altered cytoplasmic domains affect intracellular transport of the vesicular stomatitis virus glycoprotein. Cell **34**:513–524.
24. **Rottier, P. J., and J. K. Rose.** 1987. Coronavirus E1 glycoprotein expressed from cloned cDNA localizes in the Golgi region. J. Virol. **61**:2042–2045.
25. **Rottier, P. J. M., M. C. Horzinek, and B. A. M. van der Zeijst.** 1981. Viral protein synthesis in mouse hepatitis virus strain A59-infected cells: effect of tunicamycin. J. Virol. **40**:350–357.
26. **Spaan, W., D. Cavanagh, and M. C. Horzinek.** 1988. Coronaviruses: structure and genome expression. J. Gen. Virol. **69**: 2939–2952.
27. **Stern, D. F., and B. M. Sefton.** 1982. Coronavirus proteins: structure and function of the oligosaccharides of the avian infectious bronchitis virus glycoproteins. J. Virol. **44**:804–812.
28. **Sturman, L., and K. Holmes.** 1985. The novel glycoproteins of coronavirus. Trends Biochem. Sci. **10**:17–20.
29. **Tomley, F., M. Binns, M. Boursnell, and A. Mockett.** 1987. Expression of IBV spike protein by a vaccinia virus recombinant. J. Gen. Virol. **68**:2291–2298.
30. **Tooze, J., S. A. Tooze, and S. D. Fuller.** 1987. Sorting of progeny coronavirus from condensed secretory proteins at the exit from the trans-Golgi network of AtT20 cells. J. Cell Biol. **105**: 1215–1226.
31. **Tooze, S. A., J. Tooze, and G. Warren.** 1988. Site of addition of *N*-acetyl-galactosamine to the E1 glycoprotein of mouse hepatitis virus-A59. J. Cell Biol. **106**:1475–1487.
32. **Ward, J. M.** 1970. Morphogenesis of a virus in cats with experimental feline infectious peritonitis. Virology **41**:191–194.
33. **Williams, D. B., S. J. Swiedler, and G. W. Hart.** 1985. Intracellular transport of membrane glycoproteins: two closely related histocompatibility antigens differ in their rates of transit to the cell surface. J. Cell Biol. **101**:725–734.
34. **Yeo, K.-T., J. B. Parent, T.-K. Yeo, and K. Olden.** 1985. Variability in transport rates of secretory glycoproteins through the endoplasmic reticulum and golgi in human hepatoma cells. J. Biol. Chem. **260**:7896–7902.